Suppression of Spontaneous Gas Oscillations by Acoustic Self-Feedback

Tetsushi Biwa, Yoshiki Sawada, and Hiroaki Hyodo
Department of Mechanical Engineering, Tohoku University, Sendai 980-8579, Japan

Soichiro Kato
Heat and Fluid Dynamics Department, Research Laboratory, IHI corporation, Yokohama 235-8501, Japan

(Received 11 May 2016; revised manuscript received 12 September 2016; published 28 October 2016)

This paper demonstrates a method of acoustical self-feedback to suppress spontaneous gas oscillations such as those observed in combustors of gas-turbine engines. Whereas a conventional feedback system consists of electromechanical devices, the present method achieves acoustical self-feedback with a hollow tube that connects two positions of the oscillation system. A model oscillator of combustion-driven gas oscillations is designed and built to demonstrate the applicability of the self-feedback concept. Stability analysis through measurements of Q values (quality factor) of oscillations shows that the desired delay time and gain are obtained when the tube length is equal to the odd integer times half the wavelength of the anticipated acoustic oscillations.

DOI: 10.1103/PhysRevApplied.6.044020

I. INTRODUCTION

Suppressing combustion-driven gas oscillation has persisted as a goal that must be achieved for modern combustion technology using a fuel-lean premixed combustion. Premixed combustion, the full mixing of fuel and air before burning, is indispensable for the reduction of NO_x emissions in gas-turbine engines [1,2], but it is prone to the generation of thermally induced spontaneous gas oscillations that can reduce lifetimes or even destroy an engine [3]. For safety operations of aircraft and power plants, techniques to stop the oscillations [4] and to predict oscillations [5–7] are strongly demanded.

Delayed feedback is one method that can stop spontaneous oscillations. Atay [8] has theoretically analyzed a van der Pol oscillator under delayed feedback:

$$\ddot{x} + \epsilon(x^2 - 1)\dot{x} + x = \epsilon k x(t - \tau). \tag{1}$$

For small and positive ϵ, he adapted a method of averaging to show that the state with zero amplitude becomes stable when nondimensional delay time τ and feedback gain k satisfy the relation of $k \sin\tau > 1$. Suchorsky recently conducted a more detailed theoretical analysis through a method of two timing [9]. Independently of these theoretical studies, Heckl [10] experimentally attempted the delayed feedback to suppress spontaneous oscillations in a thermally driven acoustic system of *Rijke tube*, and demonstrated sound annihilation using a feedback system consisting of a microphone, a delay line, and a loudspeaker. Lang [11] applied this technique successfully to halt the oscillations induced in a test combustion chamber. Consequently, the validity of the delayed feedback has been recognized, but the complicated electromechanical feedback system, necessary to detect the pressure fluctuations instantaneously and to feedback them with controlled delay time and sufficiently large gain, would limit the practical availability in actual gas-turbine engine systems. The delayed feedback [8–13] can be expected to become a powerful and reliable tool to damp the oscillation if the practical components to build the feedback system were greatly simplified.

The objective of this study is to accomplish delayed feedback using an extremely simplified method. We have recently demonstrated the amplitude death phenomenon in coupled thermally driven gas oscillation systems. We showed that a gas-filled tube of a half wavelength can introduce sufficiently strong time-delay coupling through the difference of $\dot{x}$ terms between two systems [14]. In this study, we design and build a model oscillator that mimics one of the oscillation mechanisms in the combustion system. Then, we test a method of *self-feedback*, where the acoustic gas oscillation is fed back through the tube that connects two positions of the oscillator. We show how the linear stability of the zero-amplitude state changes with the tube length through measurements of Q values (quality factor) of oscillations. The applicability of the acoustical self-feedback is demonstrated using experiments for fundamental and second-mode oscillations of the model oscillator.

II. MODEL OSCILLATOR

A. Model equation of combustion instability

Presuming that the pressure in the combustion chamber is acoustically perturbed by heat-release fluctuations of the flame, the resulting pressure change disturbs the pressure

drop in the fuel injector, which changes the fuel-to-air ratio and which results in heat-release fluctuation delayed by time τ intrinsic to the combustion processes. This feedback loop results in self-sustained oscillations often with a frequency of some natural acoustic mode of the combustion chamber [15]. This scenario is represented by an oscillator forced by delayed feedback with the delay time τ and a certain gain G [16,17] as

$$\ddot{x} + c_0\dot{x} + \omega_0^2 x = Gx(t-\tau), \tag{2}$$

where c_0 (> 0) and ω_0 are constants. When the feedback term $Gx(t-\tau)$ is absent, the system is stable. The oscillation amplitude decays with an attenuation rate $\gamma = -c_0/2$. The feedback term, however, can change the stability of the system, as shown below.

If we assume the solution of the form $x(t) = A(t)\cos[\omega_0 t + \theta(t)]$ by introducing slow variables $A(t)$ and $\theta(t)$ while imposing a relation

$$\dot{A}\cos(\omega_0 t + \theta) - A\dot{\theta}\sin(\omega_0 t + \theta) = 0 \tag{3}$$

on $A(t)$ and $\theta(t)$, then the method of averaging [18] yields

$$\dot{A} = -\frac{c_\tau}{2}A, \tag{4}$$

with

$$c_\tau = c_0 + \frac{G}{\omega_0}\sin\omega_0\tau \tag{5}$$

and

$$\dot{\theta} = -\frac{G}{2\omega_0}\cos\omega_0\tau. \tag{6}$$

Therefore, the attenuation rate γ of the amplitude $A(t)$ becomes

$$\gamma = \frac{c_\tau}{2}, \tag{7}$$

whereas the oscillation frequency f_τ of $x(t)$ is given as

$$f_\tau = \frac{\omega_0}{2\pi} - \frac{G}{4\pi\omega_0}\cos\omega_0\tau. \tag{8}$$

The linear stability of the zero-amplitude state ($A = 0$) is determined by c_τ. If c_τ is positive, then the system is stable and the oscillation amplitude $A(t)$ decreases to zero after a time. However, if c_τ is negative, then the zero-amplitude state becomes unstable and $A(t)$ grows exponentially with time. Although it is omitted from Eq. (2) for brevity, a nonlinear term like the second term of the left-hand side in Eq. (1) prevents $A(t)$ from becoming infinitely large, which makes the system attracted to a limit cycle. Consequently, the stability limit is given as $c_\tau = 0$.

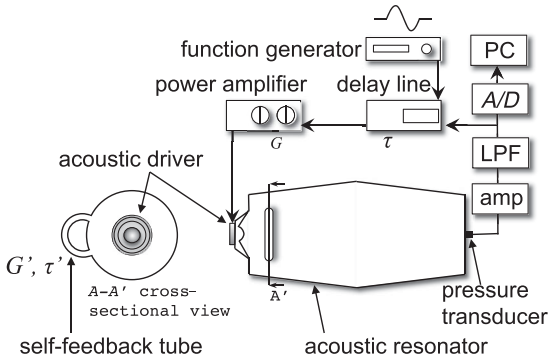

FIG. 1. Experimental setup of the model oscillator.

B. Experimental setup of the model oscillator

Figure 1 presents a schematic representation of the model oscillator constructed with simple electronics and an acoustic resonator. The barrel-shaped acoustic resonator is filled with air at ambient pressure and temperature. The axial length of the resonator is 590 mm. The largest diameter at the center is 280 mm. The smallest one at both ends is 260 mm. A pressure transducer is mounted on the center of a side plate of the resonator. An acoustic driver made of a woofer speaker is placed at the other side. As a preliminary experiment, a frequency response curve is obtained by monitoring the acoustic pressure amplitude when oscillations with various frequencies are generated by the acoustic driver. Results show that the longitudinal fundamental natural acoustic frequency f_0 [$= \omega_0/(2\pi)$] is $f_0 = 309.6$ Hz in the present acoustic resonator.

The delayed feedback is achieved in the following way. The pressure-transducer signal is put into a digital delay line via an amplifier and a low pass filter with a cutoff frequency of 1 kHz, sufficiently larger than f_0. The analogue output of the digital delay line is fed through a power amplifier to the acoustic driver. The delay time τ and the feedback gain G are tuned with the digital delay line and the power amplifier.

C. Stability curve

The stability of the model oscillator with the delayed feedback is mapped out in Fig. 2 on the plane of the gain G versus the delay time τ normalized with respect to T, where $T = 1/f_0$ denotes the acoustic period of the longitudinal fundamental natural oscillation mode. The system becomes unstable and starts to oscillate spontaneously with a sufficiently large gain G for all delay times τ that are tested, but the critical value of G, as well as the oscillation mode, depends on τ. The fundamental mode is observed in regions centered at $\tau/T = 0.8$ and 1.8, with the minimum critical value of $G = -2$ dB. The period $\tau/T = 1$ of the unstable regions reflects the τ dependence of c_τ through Eq. (5). The second mode with frequency close to $2f_0$ is observed in the regions centered about $\tau/T = 0.4$ and 1.4,

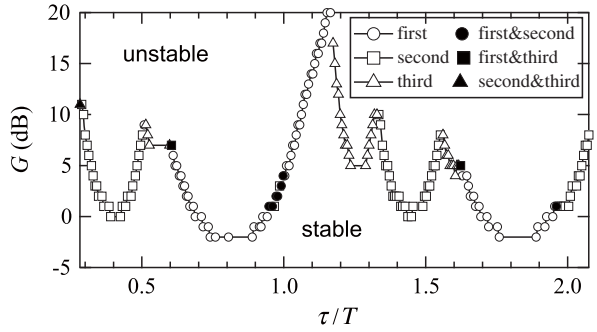

FIG. 2. Stability curve. Symbols denote the oscillation modes: The fundamental (circle), the second (square), and the third (triangle). Solid symbols are used when two oscillating modes are observed.

in addition to regions with $\tau/T \approx 1.0$ and 2.0. The stability curve of the second mode possesses a periodicity of $\tau/T = 1/2$, as we show later. The third mode with the frequency close to $3f_0$ is observed in narrow frequency regions near $\tau/T = 1.2$ and 1.6. Quasiperiodic oscillations are observed in the transition region, as shown by the solid symbols in Fig. 2.

The periodic appearance of spontaneous oscillations with varying τ is predicted to occur in a more detailed model of the lean premixed gas-turbine combustors [15]. Therefore, the present oscillator apparently shares important mechanisms with the combustion oscillations. In the following section, we first introduce a method of self-feedback to halt the fundamental oscillations generated. Then, we extend the method for application to both the fundamental and the second-mode oscillations.

III. SUPPRESSION OF OSCILLATIONS

A. Suppression mechanism of the self-feedback tube

To achieve the self-feedback of acoustic oscillations, we connect a thick-walled silicon tube with 12.7-mm internal diameter near the side plate of the resonator, as presented in Fig. 1. Acoustic oscillations at one end of the tube propagate down to the other with a delay time given by $\tau' = L/c$, where L is the tube length and c is the speed of sound. Therefore, the dynamical system shown in Eq. (2) would be modified to include an additional feedback term with the gain G' on the right-hand side as

$$\ddot{x} + c_0\dot{x} + \omega_0^2 x = Gx(t-\tau) + G'\dot{x}(t-\tau'), \tag{9}$$

where we use $\dot{x}$ instead of x based on our previous experiments [14]. This modification changes Eqs. (4) and (6) into

$$\dot{A} = -\frac{A}{2}\left(c_\tau - G'\cos\frac{2\pi L}{\lambda}\right), \tag{10}$$

$$\dot{\theta} = 2\pi f_\tau - \frac{G'}{2}\sin\frac{2\pi L}{\lambda}, \tag{11}$$

where the term $\omega_0\tau'$ has been replaced with $2\pi L/\lambda$ through the relation $\lambda = c/f_0$. Now the attenuation rate γ is given as

$$\gamma = \frac{1}{2}\left(c_\tau - G'\cos\frac{2\pi L}{\lambda}\right) \tag{12}$$

when the self-feedback is turned on. Even if c_τ is negative, the self-feedback can recover the stability of the system when L and G' are tuned to satisfy the condition

$$c_\tau > G'\cos\frac{2\pi L}{\lambda}. \tag{13}$$

The condition in Eq. (13) is rewritten as $G' > c_\tau/\cos(2\pi L/\lambda)$ and $\cos(2\pi L/\lambda) < 0$, for $c_\tau < 0$. Once the condition of Eq. (13) is satisfied, the zero-amplitude state remains stable.

B. Evaluation of stability by the Q value

To study the stability of the model oscillator, we specifically examine the Q value of oscillations because it is a nondimensional quantity that reflects the attenuation rate γ in Eq. (12). Assuming that the angular frequency of the relaxation oscillation $x(t)$ is close to the natural angular frequency ω_0, the conventional prescription of dynamics links the Q value with the attenuation rate γ as [19]

$$\frac{1}{Q} = \frac{2\gamma}{\omega_0}. \tag{14}$$

As discussed in Sec. II A, the zero-amplitude state loses its stability when γ crosses zero: when $1/Q$ becomes infinitely large.

The Q value is determined from measurements of the attenuation rate γ of the acoustic pressure $p(t)$. A tone burst voltage signal with the carrier frequency f_0 is created with a function generator and fed to a mixing port of the delay line at $t = 0$. The voltage pulse, superposed on the signal from the pressure transducer, is supplied to the acoustic driver as an excitation signal. The resulting damped oscillation of $p(t)$ is sampled using an A/D converter. The delay time is fixed to $\tau/T = 0.8$, whereas the gain G is maintained at $G = -5$ dB to keep the stability of the system consistently.

Shown in Fig. 3(a) is the temporal pressure evolution observed in the model oscillator without the self-feedback tube, where the pressure waveform is sinusoidal with exponentially decreasing amplitude. The instantaneous amplitude and the instantaneous phase are determined through the Hilbert transform of $p(t)$. The logarithmic of the instantaneous amplitude, as depicted in Fig. 3(b), is approximated as a linear function of time with using the least squares method. The attenuation rate γ is derived from the slope by considering the conversion from a base-10 logarithm to a natural logarithm. The instantaneous phase depicted in Fig. 3(c) is also approximated using a linear function of time. The oscillation angular frequency ω is

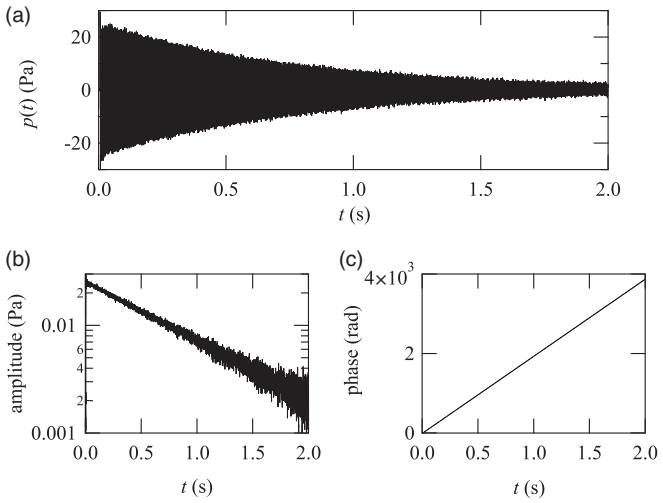

FIG. 3. Pressure oscillation excited by an acoustic pulse at $t = 0$, when $\tau/T = 0.8$ and $G = -5$ dB. From temporal pressure evolution in (a), the instantaneous amplitude (b) and instantaneous phase (c) are obtained.

obtained from the slope. From the measured pressure depicted in Fig. 3(a), we find that $\gamma = 1.25\ \mathrm{s}^{-1}$ and $f_\tau = 308.0$ Hz, being close to f_0. The value of Q is then determined as $Q = 778$ from Eq. (14).

In most cases, both the logarithmic amplitude and the phase linearly change with time, as shown in Figs. 3(b) and 3(c), but when Q reaches below about 100 because of the self-feedback tube, the envelope of $p(t)$ often shows beats during the relaxation process to zero. Although such cases engender large estimation errors of Q and f, the error sizes are still acceptable.

C. Experimental results of Q

Figures 4(a) and 4(b) show the $1/Q$ values and the oscillation frequencies f $[= \omega/(2\pi)]$ obtained for various tubes. In Figs. 4(a) and 4(b), the tube length L is normalized with respect to the wavelength $\lambda = c/f_0$. The Q value ($Q = 778$) and the oscillation frequency ($f_\tau = 308.0$ Hz) are also shown as horizontal lines in Figs. 4(a) and 4(b) for comparison when the self-feedback tube is absent. The stability of the system is undoubtedly improved by the self-feedback tube, as evidenced by the enhancement of $1/Q$ values when L/λ is close to 0.5 and 1.5. Because $\cos(2\pi L/\lambda)$ goes to -1 with these values of L/λ, this result is consistent with the attenuation rate γ in Eq. (12).

By inserting γ in Eq. (12) into Eq. (14), the inverse of the quality factor, $1/Q$, is obtained as a function of L/λ as

$$\frac{1}{Q} = \frac{1}{Q_\tau} - \frac{G'}{\omega_0}\cos\frac{2\pi L}{\lambda}, \tag{15}$$

where $Q_\tau = \omega_0/c_\tau$. The oscillation frequency f is also given from Eq. (11) in the same way as

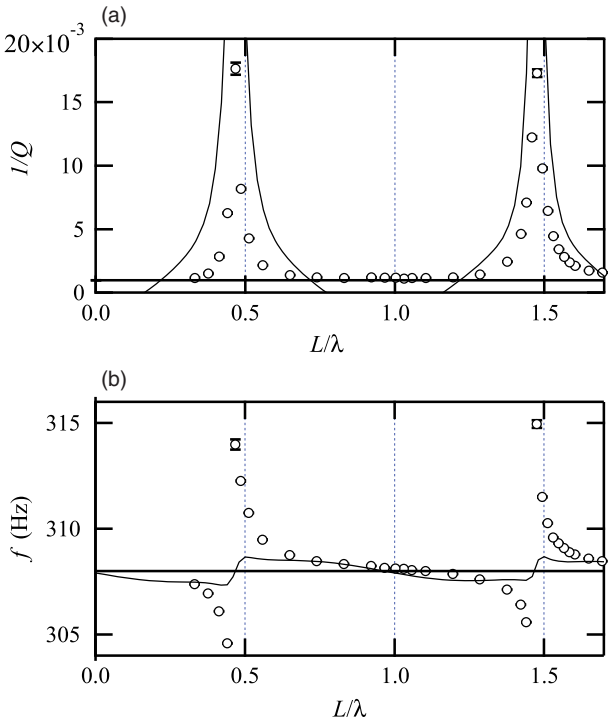

FIG. 4. The inverse of the Q value (a) and the oscillation frequency f (b) when feedback tube length L is changed. The delay time and gain are fixed at $\tau/T = 0.8$ and $G = -5$ dB. The curves, respectively, portray the reproduction of $1/Q$ and f based on the estimated gain G' through Eqs. (15) and (16).

$$f = f_\tau - \frac{G'}{4\pi}\sin\frac{2\pi L}{\lambda}. \tag{16}$$

We see that the two maxima of $1/Q$, as well as the sign changes of $f - f_\tau$, near $L/\lambda = 0.5$ and 1.5 are consistent with Eqs. (15) and (16). However, the L/λ dependences of $1/Q$ and f differ from sinusoidal functions. Therefore, to reproduce $1/Q$ and f in Figs. 4(a) and 4(b) fully, the gain G' must vary with L/λ.

Inserting Eqs. (15) and (16) into the relation $\cos^2(2\pi L/\lambda) + \sin^2(2\pi L/\lambda) = 1$ yields

$$G' = \sqrt{\omega_0^2\left(\frac{1}{Q_\tau} - \frac{1}{Q}\right)^2 + 16\pi^2(f_\tau - f)^2}. \tag{17}$$

We have evaluated G' through Eq. (17) using measured values of ω_0, Q, Q_τ, f, and f_τ, as depicted in Fig. 5. Taking aside the small differences from 0.5 and 1.5, one can say that gain G' becomes greater when tube length L is close to $(2n-1)\lambda/2$, but it remains small for other values of L, where n is an integer. Therefore, the gain G' of the self-feedback only contributes to stabilizing the system. In other words, if G' is constant as in the external feedback, then the system would become unstable when L approaches $n\lambda$.

After fitting the obtained G' to a curve given by a sum of two Lorentz curves that have peaks at $L/\lambda = 0.46$ and 1.46,

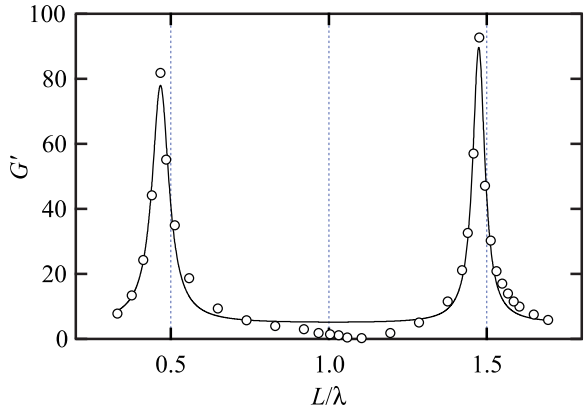

FIG. 5. Relation between the gain G' of the self-feedback and the tube length L. λ is the wavelength of the acoustic oscillations. The curve represents a fitting result to a Lorentz curve with peaks at $L/\lambda = 0.46$ and 1.46.

we calculated $1/Q$ and f through relations in Eqs. (15) and (16). Results are shown by thin curves in Figs. 4(a) and 4(b), where qualitative agreement is seen with experimental values. Because gain G' serves as a quantity characterizing the ability to suppress the oscillations, additional studies must be undertaken to ascertain methods to enhance the gain G' at particular values of L/λ.

D. Stability curve with a self-feedback tube

The stability limit is determined experimentally with varying delay times τ of the digital delay line to test the ability of the self-feedback tube. Figure 6(a) shows the stability curve when the self-feedback tube with $L/\lambda = 0.46$, together with that when the feedback tube is absent. When the delay time τ is tuned as $\tau/T = 0.8$, the system without self-feedback becomes unstable with $G \geq -2$ dB. However, when the self-feedback is adapted, the system remains stable as long as G is less than 10 dB. The resulting gain enhancement is 12 dB, which means that the system remains stable until G becomes $10^{0.6}(\approx 4.0)$ times larger than the critical value. Such improvement is also attained for the fundamental mode at $\tau/T = 1.8$.

Although the stability of the fundamental mode oscillations is improved by the self-feedback tube with $L/\lambda = 0.46$, that of the second-mode oscillations is insensitive to it. As a result, the second-mode oscillations mostly govern the stability curve in Fig. 6(a), where we can more clearly see the periodic appearance of the second mode, which is hidden in Fig. 2.

The second mode has a frequency of about $2f_0$, which means that the wavelength becomes almost half of that for the fundamental. Therefore, the tubes with $L/\lambda = 0.5, 1.5, \ldots$ for the fundamental acoustic mode are useless. Instead, the tubes with $L/(\lambda/2) = 0.5, 1.5, \ldots$ become necessary to stop oscillations. Figure 6(b) presents the stability curve when the secondary self-feedback tube

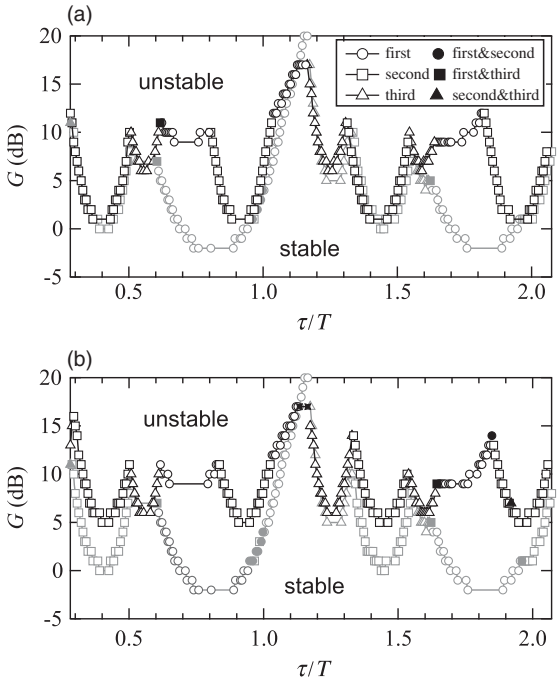

FIG. 6. Stability curves with (a) the tube with $L/\lambda = 0.46$ and (b) the two tubes with $L/\lambda = 0.46$ and 0.74. Symbols to denote the oscillation modes are the same as in Fig. 2. The stability curve shown by gray is reproduced from Fig. 2.

with $L/\lambda = 0.74$ is connected to the resonator at the same axial position as the first with $L/\lambda = 0.46$. Comparison between Figs. 6(a) and 6(b) presents that the minimum threshold values of about 0 dB at $\tau/T = 0.4$, 0.9, 1.4, and 1.9 have increased by installation of the secondary tube. As a result, the system gained its stability up to $G = 5$ dB for all the τ values.

It is clear that one should use a tube with a length equal to the odd integer times half the wavelength of the anticipated oscillation modes. In practical combustors, the natural frequency might be varied according to operating conditions. In such a case, tubes with different lengths and internal diameters would be necessary to control the delay time and the feedback gain. We plan to develop a method to apply the feedback tube in a real system.

IV. SUMMARY

We have demonstrated the suppression of spontaneous acoustic oscillations using self-feedback. Self-feedback is realized using only a tube with a length equal to the odd integer times the half wavelength of the anticipated acoustic mode. The simplicity is the advantage of the present method to the conventional delayed-feedback system.

ACKNOWLEDGMENTS

This work was supported by JSPS KAKENHI (26286073).

[1] K. Döbbeling, J. Hellat, and H. Koch, 25 years of BBC/ABB/Alstom lean premix combustion technologies, J. Eng. Gas Turbines Power **129**, 2 (2007).
[2] S. Candel, Combustion dynamics and control: Progress and challenges, Proc. Comb. Inst. **29**, 1 (2002).
[3] C. J. Goy, S. R. James, and S. Rea, in *Combustion Instabilities in Gas Turbine Engines: Operational Experience, Fundamental Mechanism, and Modeling*, edited by T. C. Lieuwen and V. Yang (Progress in Astronautics and Aerodynamics, Reston, VA, 2005), Chap. 8.
[4] D. L. Gysling, G. S. Copeland, D. C. McCormick, and W. M. Proscia, Combustion system damping augmentation with Helmholtz resonators, J. Eng. Gas Turbines Power **122**, 269 (2000).
[5] D. W. Kendrick, T. J. Anderson, W. A. Sowa, and T. S. Snyder, Acoustic sensitivities of lean-premixed fuel injectors in a single nozzle rig, J. Eng. Gas Turbines Power **121**, 429 (1999).
[6] J. Ballester and T. Garcia-Armingol, Diagnostic techniques for the monitoring and control of practical flames, Prog. Energy Combust. Sci. **36**, 375 (2010).
[7] H. Gotoda, Y. Shinoda, M. Kobayashi, Y. Okuno, and S. Tachibana, Detection and control of combustion instability based on the concept of dynamical system theory, Phys. Rev. E **89**, 022910 (2014).
[8] F. M. Atay, Van der Pol's oscillator under delayed feedback, J. Sound Vib. **218**, 333 (1998).
[9] M. K. Suchorsky, S. M. Sah, and R. H. Rand, Using delay to quench undesirable vibrations, Nonlinear Dyn. **62**, 407 (2010).
[10] M. Heckl, Active control of the noise from a Rijke tube, J. Sound Vib. **124**, 117 (1988).
[11] W. Lang, T. Poinsot, and S. Candel, Active control of combustion instability, Combust. Flame **70**, 281 (1987).
[12] M. Ciofini, A. Labate, R. Meucci, and M. Galanti, Stabilization of unstable fixed points in the dynamics of a laser with feedback, Phys. Rev. E **60**, 398 (1999).
[13] A. Ahlborn and U. Parlitz, Controlling dynamical systems using multiple delay feedback control, Phys. Rev. E **72**, 016206 (2005).
[14] T. Biwa, S. Tozuka, and T. Yazaki, Amplitude Death in Coupled Thermoacoustic Oscillators, Phys. Rev. Applied **3**, 034006 (2015).
[15] T. Lieuwen, H. Torres, C. Johnson, and B. T. Zinn, A mechanism of combustion instability in lean premixed gas turbine combustors, J. Eng. Gas Turbines Power **123**, 182 (2001).
[16] T. Yi and E. J. Gutmark, Online prediction of the onset of combustion instability based on the computation of damping ratios, J. Sound Vib. **310**, 442 (2008).
[17] K. Balasubramanian and R. I. Sujith, Thermoacoustic instability in a Rijke tube: Non-normality and nonlinearity, Phys. Fluids **20**, 044103 (2008).
[18] J. L. Hale, Averaging methods for differential equations with retarded arguments and a small parameter, J. Differ. Equations **2**, 57 (1966). See also, Steven Strogatz, *Nonlinear Dynamics and Chaos: With Applications to Physics, Biology, Chemistry, and Engineering* (Westview Press, Cambridge, MA, 2000); Robert C. Hilborn, *Chaos and Nonlinear Dynamics: An Introduction for Scientists and Engineers* (Oxford University Press, New York, 1994).
[19] A. P. French, *Vibrations and Waves* (W. W. Norton Company, New York, 1971).